Title

Rational Design of RNA Editing Guide Strands: Cytidine Analogs at the Orphan Position

Journal

Journal of the American Chemical Society, 143(18)

ISSN

0002-7863

Authors

Doherty, Erin E

Wilcox, Xander E

van Sint Fiet, Lenka

et al.

Publication Date

2021-05-12

DOI

10.1021/jacs.0c13319

Peer reviewed

HHS Public Access

Author manuscript

J Am Chem Soc. Author manuscript; available in PMC 2021 November 22.

Published in final edited form as:

J Am Chem Soc. 2021 May 12; 143(18): 6865–6876. doi:10.1021/jacs.0c13319.

Rational Design of RNA Editing Guide Strands: Cytidine Analogs at the Orphan Position

Erin E. Doherty,
Department of Chemistry, University of California, Davis, California 95616, United States

Xander E. Wilcox,
Department of Chemistry, University of California, Davis, California 95616, United States

Lenka van Sint Fiet,
ProQR Therapeutics, 2333 CK Leiden, The Netherlands

Cherie Kemmel,
ProQR Therapeutics, 2333 CK Leiden, The Netherlands

Janne J. Turunen,
ProQR Therapeutics, 2333 CK Leiden, The Netherlands

Bart Klein,
ProQR Therapeutics, 2333 CK Leiden, The Netherlands

Dean J. Tantillo,
Department of Chemistry, University of California, Davis, California 95616, United States

Andrew J. Fisher,
Department of Chemistry, University of California, Davis, California 95616, United States

Department of Molecular and Cellular Biology, University of California, Davis, California 95616, United States

Peter A. Beal
Department of Chemistry, University of California, Davis, California 95616, United States

Abstract

Adenosine Deaminases Acting on RNA (ADARs) convert adenosine to inosine in double stranded RNA. Human ADARs can be directed to predetermined target sites in the transcriptome by complementary guide strands, allowing for the correction of disease-causing mutations at the RNA

Corresponding Author:Peter A. Beal – Department of Chemistry, University of California, Davis, California 95616, United States; pabeal@ucdavis.edu.

Supporting Information

The Supporting Information is available free of charge at https://pubs.acs.org/doi/10.1021/jacs.0c13319.
Crystallography data, oligonucleotide sequences, DFT calculations, and editing experiments, including Figures S1–S9 and Tables S1–S6 (PDF)

Complete contact information is available at: https://pubs.acs.org/10.1021/jacs.0c13319

The authors declare the following competing financial interest(s): E.E.D., L.v.S.F., C.K., J.J.T., B.K., and P.A.B. have filed a patent application on this work. P.A.B. is a consultant for Agios Pharmaceuticals, ProQR Therapeutics and Beam Therapeutics. P.A.B. has ownership interest in Beam Therapeutics. L.v.S.F., C.K., J.J.T., and B.K. are employees and shareholders of ProQR Therapeutics.

level. Here we use structural information available for ADAR2-RNA complexes to guide the design of nucleoside analogs for the position in the guide strand that contacts a conserved glutamic acid residue in ADARs (E488 in human ADAR2), which flips the adenosine into the ADAR active site for deamination. Mutating this residue to glutamine (E488Q) results in higher activity because of the hydrogen bond donating ability of Q488 to N3 of the orphan cytidine on the guide strand. We describe the evaluation of cytidine analogs for this position that stabilize an activated conformation of the enzyme-RNA complex and increase catalytic rate for deamination by the wild-type enzyme. A new crystal structure of ADAR2 bound to duplex RNA bearing a cytidine analog revealed a close contact between E488, stabilized by an additional hydrogen bond and altered charge distribution when compared to cytidine. In human cells and mouse primary liver fibroblasts, this single nucleotide modification increased directed editing yields when compared to an otherwise identical guide oligonucleotide. Our results show that modification of the guide RNA can mimic the effect of hyperactive mutants and advance the approach of recruiting endogenous ADARs for site-directed RNA editing.

Graphical Abstract

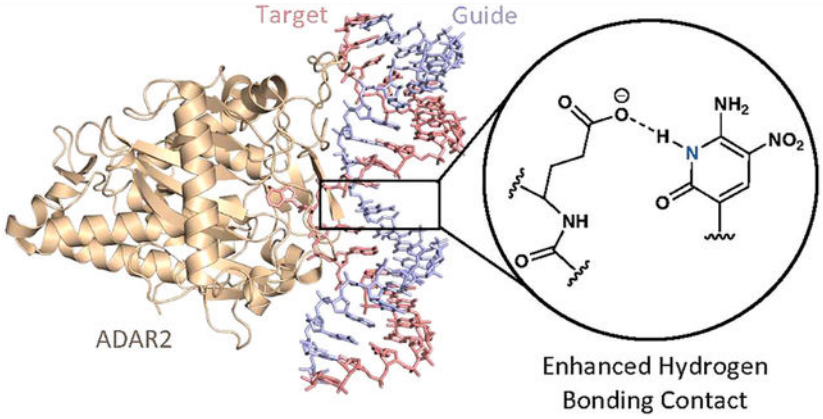

INTRODUCTION

Enzymes that can be programmed to site-specifically alter nucleic acids offer a promising platform for the correction of disease-causing mutations.[1–3] Adenosine Deaminases Acting on RNA (ADARs) have been used to deaminate target adenosines to inosine in double stranded RNAs.[4] Inosine is recognized as guanosine during translation, meaning that the ADAR reaction has therapeutic potential for the correction of pathogenic G-to-A point mutations. Commonly, RNA guided enzymes are localized to a target sequence by nucleic acid hybridization.[5–8] Since ADARs only act on double stranded RNA, they can be directed to target adenosines using a guide oligonucleotide. This technology boasts the same programmable nature as Cas-mediated DNA editing, but holds some possible advantages for clinical applications. The effects of RNA editing are transient, meaning that any off-target edits do not result in a permanent change to the genome. On the other hand, unlike DNA editing, RNA editing therapeutics would require continuous administration.[9] However, RNA editing provides a reversible and tunable solution. In addition, base-editing by ADARs does not induce double strand breaks and is not restricted to a particular phase of the cell cycle.[3]

Also, immunogenicity of bacterial-derived Cas enzymes and delivery vectors has led to concerns over the safety and efficacy of their use in gene therapy.[10–12]

These delivery barriers and immune stimulation issues have sparked interest in systems that employ endogenous human enzymes, including ADARs, to edit disease-relevant nucleic acids.[9,13,14] Until recently, the primary approach to site-directed RNA editing by ADARs was reliant on the overexpression of engineered enzymes and codelivery of a guide RNA.[15–18] However, ectopic expression of ADARs leads to increased levels of off-target editing[13] and has been shown to induce toxicity in mice.[14] Additional strategies have been reported that establish the use of endogenous ADARs for RNA editing.[9,13,14] However, such strategies have required long guide RNAs and still offer room for improvement in efficiency and specificity. Here, we describe efforts to design nucleobase modifications for short guide oligonucleotides to increase A-to-I editing efficiency at target sites using endogenous ADARs.

RESULTS

Orphan Base Analogs That Mimic a Hyperactive ADAR2 Mutant.

When ADARs edit target adenosines, the edited base is flipped into the enzyme active site leaving behind an “orphan base.”[20] In the preferred pairing context for ADARs, an A–C mismatch, this creates an unpaired cytidine.[21,22] Structures of ADAR2 deaminase domain bound to RNA revealed that glutamic acid residue 488, in the highly conserved flipping loop of the enzyme, occupies the space vacated by the reacting adenosine.[20] The enzyme stabilizes this base-flipped conformation through a suspected hydrogen bond between the protonated side chain of E488 and N3 of the orphan cytidine (Figure 1a; Figure 2b).[20] Previously, it had been shown that a single mutation at residue 488 from glutamic acid to glutamine leads to enzyme hyperactivity, with up to a 60-fold increase in deamination rate constant for some substrates.[23] The structures of the deaminase domain of both wild-type and hyperactive ADAR2 bound to dsRNA have been solved and reveal that the positioning of residue 488 is nearly superimposable between the two enzymes (Figure 1a,b).[20] It appears that ADAR2 E488Q makes the same hydrogen bonding contact between the side chain and N3 of the orphan cytidine. Importantly, the carboxyamide of the glutamine side chain can function as a hydrogen bond donor independent of pH in the physiologically relevant range. This is thought to be the reason for the hyperactivity of ADAR2 E488Q (Figure 2a).[20,23] Indeed, recently described pH effects on the deamination rates for wild-type and E488Q mutant ADAR2 support this hypothesis.[24]

These observations inspired us to test orphan base analogs capable of hydrogen bonding with the wild-type E488 residue in a protonation-independent manner. By stabilizing the same contact made by the mutant enzyme, this may allow wild-type ADAR2 to elicit a similar hyperactive effect. Chemically modifying the guide RNA to enhance this base-flipping contact, instead of using an enzyme mutation, could enhance substrate reactivity toward endogenous ADAR enzymes. To test this idea, we incorporated cytidine analogs with hydrogen bond donors at N3 into the orphan position of guide RNAs. The orphan base analogs 8-oxo-2′-deoxyadenosine (8-oxodA), 2′-deoxypseudoisocytidine (dpiC),[25–27] and 6-amino-5-nitro-3-(1′-β-D-2′-deoxyribofuranosyl)-2(1*H*)-pyridone (referred to as 2′-deoxy

Benner's base Z or dZ)[28] were chosen due to their hydrogen bond *donor–donor–acceptor* patterns (Table 1) which retain structural features involved in ADAR2-RNA contacts, while altering the hydrogen bonding capability at N3 (Figures 2c, S1).[20] The use of 2′-deoxynucleotides in these studies was due to their ready availability and metabolic stability in cell-based directed editing assays compared to their ribonucleotide counterparts. The use of 2′-deoxy, 2′-O-methyl and phosphorothioate modifications in therapeutic oligonucleotides is a common strategy to increase cellular stability.[29,30]

A fluorescence-based assay shows guide RNA-induced changes in base-flipping.

To study the effect of these orphan base analogs on base-flipping by ADAR2, we used a previously described assay that monitors changes in the fluorescence of a 2-aminopurine (2-AP)-labeled RNA.[23,31] 2-AP is highly fluorescent as part of a single-stranded oligonucleotide, but its fluorescence is quenched when it is part of a duplex structure. This has made 2-AP useful as a probe for base-flipping by nucleic acid modifying enzymes, including ADAR2.[31–33] By incorporating 2-AP at the edited position of a target RNA, fluorescence intensity (FI) can be monitored, allowing for quantification of base flipping by ADAR2.[31] Previously, this assay has been used to examine the effect of ADAR2 mutations on base-flipping, where it was shown that ADAR2 E488Q has a 2.1-fold increase in FI compared to ADAR2 WT.[23] In binding assays, the affinity of ADAR2 WT and E488Q for target RNA was shown to be similar, suggesting that the increase in deamination rate was attributed to the enhanced base-flipping ability of the enzyme.[23] In this study, instead of comparing the effect of ADAR2 mutations, we examined the effect of guide strand modifications on base-flipping.

We incorporated 2-AP into the R/G editing site of a 28-nt RNA derived from the *GRIA2* pre-mRNA, a well-studied ADAR2 substrate.[23,31] The 2-AP containing target RNA was paired with 28-nt orphan base-modified guide RNAs, where the editing site nucleotide was paired across either dC, dZ, or dpiC (Figure 3a). FI measurements were taken of the RNA substrate in the absence of protein, and the change in fluorescence upon the addition of ADAR2 was examined. The enzyme-dependent change in fluorescence observed with different guide RNAs indicated that base-flipping was preferentially enhanced when ADAR2 wild-type (WT) was paired with an RNA containing dZ in the orphan position (Figure 3; Table S1). The normalized fluorescence enhancement increased 3.9-fold when ADAR2 WT was paired with dZ containing RNA as opposed to the unmodified orphan base dC (Figure 3b; Table S1). However, 2′-deoxypseudoisocytidine (dpiC) failed to show an enhancement in base-flipping compared to dC (Figure S2).

We also examined the change in 2-AP fluorescence for substrates in the presence of ADAR2 E488Q. It was previously shown that ADAR2 E488Q exhibits a greater extent of base-flipping than the wild-type enzyme.[23] We found that this held true for guide RNAs containing 2′-deoxycytidine in the orphan position. For guide RNAs containing dC, a 2.4-fold greater increase in fluorescence was observed when ADAR2 E488Q was added to the fluorescent substrate compared to wild-type (Table S1). However, we found that the enzyme preference was reversed for RNAs containing dZ. For guide RNAs containing dZ, base-flipping was reduced by over 4-fold in the presence of ADAR2 E488Q (Figure 3).

Interestingly, guide RNAs containing dpiC did not show a preference for either enzyme (Figure S2b; Table S1). This could be due to the ability of the pseudoisocytidine base to tautomerize such that N3 would be either a hydrogen bond donor or acceptor (Figure S2c).[34] These results suggest that base-flipping by ADAR2 is most efficient when a complementary hydrogen bond *donor–acceptor* pair exists between residue 488 and N3 of the orphan base.

Cytidine Analogs increase rate of A-to-I editing *in vitro*.

While examining how amino acids within the ADAR2 enzyme mediate editing preferences, Kuttan and Bass observed a positive correlation between catalytic rate and enhanced base-flipping ability.[23] Therefore, orphan analogs that stabilize the base-flipped conformation of the protein-RNA complex should also stimulate catalysis. To test this idea, cytidine analogs examined in the base-flipping assay were incorporated into 29-nt guide RNAs and hybridized to a 320-nt RNA sequence derived from a mouse model of Hurler syndrome (Figure 4a).[35,36] Hurler syndrome is the most severe type of α-l-iduronidase enzyme deficiency, caused by mutations in the *IDUA* gene. The most common of these is the nonsense mutation W402X, which is modeled by the W392X mutation in the mouse *Idua* gene.[35] This TGG-to-TAG mutation can be reversed by site-directed RNA editing with ADAR enzymes. Qu et al. have shown that RNA guides can recruit endogenous ADARs to edit the *IDUA* pre-mRNA and mRNA, restoring α-liduronidase catalytic activity in patient-derived W402X fibroblasts.[9] The base-flipping study described above suggests that guide RNAs containing dZ may enhance ADAR2 activity. Therefore, we compared duplexes where the orphan base was either dC, dZ, dpiC, or 8-oxodA in an *in vitro* deamination reaction with ADAR2 wild-type in single-turnover conditions (Figures 4, S3a). The combination of ADAR2 wild-type and an RNA substrate containing 2′-deoxycytidine (dC) led to a deamination reaction where k_{obs} = 1.2 ± 0.1 min^{-1} (k_{rel} = 1), while the same protein deaminated the substrate containing an orphan dZ 3-fold faster (k_{obs} = 3.6 ± 0.3 min^{-1}, k_{rel} = 3.0) (Figure 4b; Table 1). This result demonstrates the important role that the E488-orphan base contact performs in enabling efficient deamination by the wild-type enzyme. The A-dpiC substrate also showed a significant increase in reaction rate (k_{obs} = 1.6 ± 0.1 min^{-1}, k_{rel} = 1.3). The rate enhancement was not as large as with the A-dZ substrate, which could be due to its ability to present either a hydrogen bond donor or acceptor at N3 through tautomerization (Figure S2c; Table 1). However, when the RNA substrate contained 8-oxodA in the orphan position, the rate of reaction significantly decreased to k_{obs} = 0.4 ± 0.2 min^{-1} (k_{rel} = 0.3) (Table 1). This may be a result of 8-oxodA adopting the *anti* conformation instead of the *syn* conformation that is required to present the hydrogen bond *donor–donor–acceptor* face to contact residue 488.[37]

Notably, the ADAR2 E488Q enzyme shows an opposite substrate preference from ADAR2 WT. The wild-type enzyme more efficiently deaminates adenosines paired across dZ, while ADAR2 E488Q prefers substrates containing the orphan base dC (Figure 4; Table S2). This illustrates that k_{obs} is greater when a hydrogen-bond *donor–acceptor* pair is present between N3 of the orphan base and residue 488. This also mirrors the result of the base-flipping assay, showing that orphan base modifications that enhance base-flipping also provide an increase in editing rate.

Although there are currently no published high-resolution structures of ADAR1 to inform guide RNA design, it is known that ADAR1 E1008 corresponds to E488 in ADAR2.[38] Similarly, a glutamate to glutamine mutation in this residue of ADAR1 (E1008Q) shows higher activity than the wild-type enzyme.[39] Therefore, replacing the orphan base with an N3 hydrogen bond donor may increase the reaction rate for ADAR1 as well as ADAR2. To test this idea, we compared duplexes where the orphan base was either dC or dZ in an *in vitro* deamination reaction with ADAR1 p110 wild-type in single-turnover conditions (Figures 4c, S3b). The combination of ADAR1 p110 and the A-dC substrate led to a reaction where k_{obs} = 0.060 ± 0.008 min^{-1} (k_{rel} = 1) (Table 1). When the RNA substrate instead contained dZ in the orphan position, the rate of reaction increased to k_{obs} = 0.19 ± 0.02 min^{-1} (k_{rel} = 3.2). This result indicates that the rate of reaction for the ADAR1 enzyme can also be enhanced by including an N3 hydrogen bond donor analog in the orphan position of the guide RNA.

As seen by others, the use of ADAR2 E488Q *in vitro* resulted in significantly greater levels of off-target editing (Figure S4; Table S3).[14,18,19,40,41] The presence of glutamate at the 488 position in wild-type ADAR2 is likely important in editing regulation, providing a compromise between editing efficiency and specificity.[23] In contrast with ADAR2 E488Q, which not only enhances the rate of reaction but also results in editing promiscuity,[14,18,40,41] the dZ modification did not lead to higher levels of bystander editing (Figure S4; Table S3).

High-resolution structure reveals ADAR-dZ contacts.

The enhanced base-flipping and *in vitro* reaction rate stimulated by dZ containing substrates inspired the use of X-ray crystallography to examine the specific contacts made by the dZ base. The nucleoside analog 8-azanebularine has been shown to enable these structural studies, by trapping the ADAR2-RNA complex in the base-flipped conformation.[20,42,43] We synthesized a target RNA containing 8-azanebularine in place of the reactive adenosine, paired across a guide RNA containing dZ at the orphan position (Figure 5a). The crystal structure of human ADAR2 deaminase domain WT (hADAR2d WT)/dZ was determined at 2.5 Å resolution (Table S4).

As observed in previous structures, the asymmetric unit contained one deaminase domain bound to dsRNA (Chain A) dimerized with a dsRNA-free deaminase domain (Chain D).[44] Expectedly, the 8-azanebularine is flipped out of the duplex into the protein active site and the base-flipping residue E488 interacts with the orphan base dZ through hydrogen bonds from both side chain and main-chain atoms. The presence of the dZ base was confirmed by deleting the nitro group at position 5 from the structural model, running a round of refinement, and analyzing the 2Fo–Fc and Fo–Fc maps. Deleting the nitro group resulted in a strong peak of positive Fo–Fc difference electron density where the nitro group would lie (Figure S5a). Reintroduction of the nitro group results in a loss of the positive Fo–Fc difference density (Figure S5b).

Interestingly, the E488-dZ pair makes an additional interaction where the carboxylate of E488 forms a 2.80 Å bifurcated hydrogen bond with the exocyclic amine at the 4-position and the N3 of the orphan dZ (Figure 5b). Given that dZ provides an additional hydrogen bond donor to the E488 acceptor that cytidine lacks, the E488-dZ pair likely stabilizes

the base-flipped conformation. In previous structures this stabilization required either protonation at N3 (Figure 2b) or a mutant Q488 flipping residue (Figure 2a) to provide a hydrogen bond donor.

The presence of the nitro group on the dZ base prompted us to question if the charge distribution of the Watson–Crick face was contributing to enhanced stability of the flipped conformation. To investigate this, density functional theory (DFT) calculations of Benner's base Z and cytosine were conducted using the M06–2X/6–311+g(2d,p) method. These calculations suggest that the partial charge of the *donor–donor–acceptor* face of the dZ base adopts a more positive charge (Figure S6a) than the *donor–acceptor–acceptor* face of cytosine (Figure S6b). This suggests that the electrostatic interaction between the partial positive face of dZ and the carboxylate of E488 may provide additional favorable interaction energy to the base-flipped conformation.

The deaminase domain of ADAR2 is known to make several contacts with the 2′-hydroxyl of the ribose sugars. Given that the orphan dZ nucleotide lacks a 2′-hydroxyl, we sought to observe the consequence of losing this interaction. Typically, R510 forms a hydrogen bond with the 2′-hydroxyl of the orphan nucleotide and a previous 2.80 Å resolution structure (PDB ID: 6VFF) shows an additional hydrogen bond to a nearby water molecule (Figure S7a).[44] While direct contact to the orphan dZ was not observed in this structure, R510 interacts with the neighboring cytosine through a water-mediated hydrogen bonding network. The hydrogen bonding network links R510 to two successive water molecules (at 2.6 and 3.3 Å, respectively) and ultimately to the carbonyl oxygen at the 2-position of the neighboring cytosine at 3.0 Å (Figure S7b).

Site-directed RNA editing in human cells with overexpressed ADAR2 is increased by the dZ modification.

Our *in vitro* findings suggested that directed A-to-I editing by wild-type human ADARs could be enhanced with the use of dZ in guide oligonucleotides. To determine if this modification could provide editing enhancement in human cells, we synthesized a 39-nt guide oligonucleotide to direct editing by ADAR2 wild-type to the 3′-UTR of the endogenous *RAB7A* RNA present in HEK293T cells. This target was used previously in directed-editing experiments and was chosen due to the presence of an adenosine within the optimal 5′-UAG-3′ flanking sequence for ADAR2 (Figure 6a).[42,45,46] The guide strand contained 2′-*O*-methyl and phosphorothioate modifications to increase cellular stability and prevent bystander editing,[42,47–50] as well as either dC or dZ opposite the target adenosine. HEK293T cells were transfected with either dC- or dZ- containing guide oligonucleotide, and a plasmid for ADAR2 overexpression.

Guide oligonucleotide was required to observe editing at the *RAB7A* target, and no editing was observed without ADAR2 overexpression (Figure 6b; Table S5). The lack of editing without ADAR2 overexpression is likely due to the relatively low levels of ADAR expression in HEK293T cells.[51] Efficient directed editing in these cells has previously required either plasmid transfection or stable overexpression (e.g., Flip-In-T-Rex).[13,42,52] Transfection with the orphan dC guide oligonucleotide resulted in editing levels of 18% ± 4%, while transfection of the dZ guide oligonucleotide increased target editing levels to

32% ± 6% (Figure S8; Table S5). This single nucleotide change was able to induce an approximately 1.8-fold increase in editing of an endogenous target.

Directed editing with endogenous ADAR is enhanced by the dZ orphan nucleotide.

The enhancement of cellular editing using overexpressed ADAR2 suggested that use of the dZ orphan nucleotide in engineered guide strands might also amplify editing by endogenous ADARs (i.e., without ADAR overexpression). To test this idea, we synthesized guide oligonucleotides containing either dC or dZ, in addition to 2′-*O*-methyl and phosphorothioate modifications, to be tested in different sequence contexts with endogenous ADARs (Figure 7; Table S6).

Editing was performed in mouse primary liver fibroblast cells isolated from homozygous *Idua-W392X* mice on a C57BL/6 background. These cells served as a mouse model for Hurler Syndrome, carrying the disease-associated G-to-A mutation in the *Idua* gene.[35] Editing was quantified by digital droplet PCR (ddPCR), and no editing was seen in conditions without transfection, with a transfection lacking guide oligonucleotide, or using a scrambled sequence oligonucleotide (Table S7). Transfection with 100 nM control guide strand bearing dC at the orphan position induced 6 ± 2% editing at the *Idua* target site whereas a similar guide with dZ at the orphan position induced 15 ± 5% editing (Figure 7b; Table S6). Thus, compared to a guide oligonucleotide that was otherwise identical, the dZ containing guide produced 2.5-fold higher editing levels with endogenous ADAR.

Finally, directed editing was carried out on the *APP* transcript in human retinal pigment epithelium (ARPE-19) cells. The *APP* transcript was chosen as a model due to its ubiquitous expression in wild-type cells and the presence of an adenosine within a preferred sequence context for ADAR editing. We synthesized guide oligonucleotides containing either dC or dZ to target an adenosine in an AUA codon of Ile 712 thus creating the Ile to Met amino acid change within the γ-secretase cleavage site of *APP*. We again used ddPCR to quantify the editing of *APP* mRNA. As shown in Figure 7d, the 19 ± 2% *APP* RNA editing was achieved in ARPE-19 cells by transfection of 100 nM guide strand containing dZ orphan nucleotide, while only 5.8 ± 0.8% was measured for the guide strand containing dC with otherwise identical sequence and chemical modifications (Figure 7c, Table S6). Thus, again a 3.3-fold increase in editing was achieved by a dZ containing guide strand when compared to an identical but dC containing guide strand. No editing of *APP* was observed after transfection of the scrambled guide strand, no guide strand, or without transfection. Together, these experiments demonstrate that the enhancement of directed editing via endogenous ADARs by the dZ orphan nucleotide is not target RNA, sequence, or cell specific.

DISCUSSION

The use of endogenous ADARs represents a potentially safer strategy for targeting RNA and has been shown to substantially reduce levels of off-target edits, when compared to enzyme overexpression.[14] However, native ADARs typically exhibit lower levels of editing, inspiring strategies to engineer guide RNAs that overcome this barrier. Previously, Merkle et al. appended a hairpin derived from a native ADAR2 substrate to create ~60–95 nt chemically modified guides that recruit endogenous ADARs.[13] Katrekar and co-workers

also utilized a recruitment domain strategy, which they linked to long antisense domains.[14] In the LEAPER system, Qu et al. used 70–151 nt guide RNAs with A–C mismatches at the target site to direct editing by endogenous ADARs to a specific position within the resulting dsRNA.[9] Both Katrekar and Qu opted to genetically encode their guide RNAs as opposed to transfecting chemically modified guide oligonucleotides.[9,14] These studies have established the feasibility of an endogenous ADAR editing platform that only requires delivery of a guide RNA. However, limitations to each of these approaches still exist. The length of these guide oligonucleotides can lead to off-targets within the long double stranded region formed on the target transcript, or through partial base pairing of the guide to off-target transcripts, although the guide oligonucleotides were restricted to these lengths as to overcome insufficient editing levels.[9] Long antisense domains have also been associated with a decrease in target mRNA levels through an RNAi-like effect.[14,19] In addition to optimizing the length and sequence of guide oligonucleotides, chemical modification of ADAR guide RNAs (2′-*O*-methylations, phosphorothioates, locked nucleic acid) has been employed to improve cellular stability and binding kinetics and to reduce off-target editing.[13] Previous efforts have focused on recruitment and binding of endogenous ADARs, but the need remains for guide RNA modifications that specifically enhance catalysis. Here, we described nucleotide modifications that are able to enhance *in vitro* deamination kinetics when paired across a target adenosine (dZ and dpiC), and a single nucleotide modification (dZ) that ultimately more than doubled editing yield via endogenous ADARs.

The orphan position of guide oligonucleotides is known to play an important role in ADAR editing. Positioning a cytidine opposite the target A to generate an A–C mismatch is a widely used technique and is shown to increase ADAR reaction rates *in vitro*.[22,31] This rate enhancement has been attributed to the stability of the resultant base pair (I–C > I–U) post deamination.[22] However, we sought to examine how orphan base modifications can influence base-flipping to alter the reaction rate. The ADAR2 E488Q mutant is able to dramatically increase the deamination rate for an abundance of substrates without a significant change in binding affinity, owing to an enhancement in base-flipping.[23] Our *in vitro* studies confirm that this enhancement is due to an important hydrogen bonding contact between N3 of the orphan base and residue 488 (Figure 2a,b). Therefore, we sought to increase the editing efficiency of wild-type ADAR2 by engineering the guide RNA to fulfill this same contact (Figure 2c). We identified cytidine analogs that retained other ADAR2-RNA contacts, while offering hydrogen bond donation at N3. Yang et al. had previously reported an artificially expanded genetic information system (AEGIS) in which they designed purine-pyrimidine nucleobase pairs that retain standard geometry, while rearranging hydrogen bond *donor–acceptor* groups.[28] Our interest was in the “Z” nucleobase reported by the Benner group: a pyrimidine *donor–donor–acceptor*. In contrast with cytosine —a pyrimidine *donor–acceptor–acceptor*—this base offers hydrogen bond donation at N3.

Our analysis of base-flipping with different combinations of orphan base and either ADAR2 or ADAR2 E488Q furthered the understanding of protein–RNA contacts required for base-flipping. Base-flipping efficiency was greatest when there was a hydrogen bond *donor–acceptor* pair between N3 of the orphan base and the side chain of residue 488. Consequently, base-flipping for wild-type ADAR2 was greatest when paired with a substrate containing dZ (Figure 3; Table S1). Kuttan and Bass had previously demonstrated a positive

correlation between the catalytic rate and base-flipping ability of ADAR2 mutants.[23] Correspondingly, we observed that the dZ modification which enhanced base-flipping also resulted in greater *in vitro* deamination rates (Figure 4; Table S2). The high-resolution crystal structure of ADAR2 deaminase domain bound to a dZ-containing RNA allowed us to explore the structural basis of this improvement. As intended, the E488 residue formed a close hydrogen bonding interaction with the dZ base (Figure 5).

We have shown that the dZ modification can be used to increase editing efficiency in mouse and human cells. A potential advantage of using orphan C analogs in guide oligonucleotides designed to promote directed RNA editing resides in the avoidance of off-target editing associated with the use of hyper-editing ADAR2 mutants. Ultimately, we showed that guide oligonucleotides containing dZ enhance editing by endogenous ADARs for two targets (up to 3.3-fold) when compared to an otherwise identical guide containing dC at the orphan position (Figure 7). The use of dZ in the orphan position of guide RNAs represents a general approach to increase ADAR editing efficiency, having demonstrated success in multiple sequence contexts. In addition, it is compatible with a range of other chemical modifications (2′-*O*-methyl, phosphorothioate). Therefore, this approach could be combined with other methods used for endogenous ADAR recruitment and editing efficiency (chemical modifications for cellular stability, recruitment domains, lengthening of the guide oligonucleotide, etc.) to provide additional increases in editing efficiency.[9,13,14] In addition, positioning of the chemical modifications and the relative location of the orphan base within the guide RNA can be further optimized. Our method faces similar limitations as other chemically modified ADAR guides, in that they are not genetically encodable and must be delivered to target tissues. However, targeted delivery of oligonucleotides is becoming more feasible, as demonstrated by recent successes in the delivery of chemically modified oligonucleotides to the liver.[53] In addition, different RNA substrates demonstrate varying levels of rate enhancement with the use of ADAR2 E488Q.[23] Since the mechanism of rate enhancement by the dZ base likely mimics that of the mutant enzyme, it remains to be seen whether this strategy will be useful for substrates and sequence contexts that are not affected by mutation of the base-flipping residue to glutamine. Furthermore, we have yet to explore fully the utility of this orphan modification when the target adenosine is not within the context of the ideal nearest neighbors for ADARs.[46] This work is ongoing in our laboratory.

CONCLUSION

RNA editing presents a potentially safer technology than Cas-based genome editing for therapeutic applications. In addition, the use of endogenous RNA editing enzymes, such as the ADARs, can minimize barriers associated with off-target editing and enzyme delivery. These strategies require the use of guide strands that can lead to efficient directed editing. Therefore, guide strand optimization is an active area of research. Here we described the use of a modified nucleotide at the orphan position of a guide strand that mimics the effect of an activating mutation in the ADAR enzymes. Benner's dZ nucleotide (6-amino-5-nitro-3-(1′-β-D-2′-deoxyribofuranosyl)-2(1*H*)-pyridone) presents a hydrogen bonding pattern optimal for interaction with a glutamate residue present on the ADAR flipping loop, leading to increased deamination rates *in vitro*. A crystal structure of ADAR2 deaminase domain

bound to RNA containing dZ showed the novel protein–RNA contact in atomic resolution. Finally, this single nucleotide modification led to a significant increase in editing yields with endogenous ADAR in human cells and mouse primary liver fibroblasts, when compared to an otherwise identical guide oligonucleotide. These studies lay the groundwork for additional rational design of optimized ADAR guide strands.

MATERIALS AND METHODS

General Biochemical Procedure.

Molecular-biology-grade bovine serum albumin (BSA) and RNase inhibitor were purchased from New England BioLabs. SDS-polyacrylamide gels were visualized with a Molecular Dynamics 9400 Typhon phosphorimager. Data were analyzed with Molecular Dynamics ImageQuant 5.2 software. All MALDI analyses were performed at the University of California, Davis Mass Spectrometry Facilities using a Bruker UltraFlextreme MALDI TOF/TOF mass spectrometer. Oligonucleotide masses were determined with Mongo Oligo Calculator v2.08. Oligonucleotides for sequencing and PCR were purchased from Integrated DNA Technologies. RNA containing 2-aminopurine was purchased from Dharmacon and purified as described below. All other oligonucleotides were synthesized as described below.

Synthesis of Oligonucleotides.

Chemical synthesis for all oligonucleotides was performed using an ABI 394 synthesizer. Pseudoisocytidine (piC) deoxyribonucleoside phosphoramidite and 8-azanebularine ribonucleoside phosphoramidite were purchased from Berry & Associates, Inc. Benner's base Z was purchased from FireBird Biomolecular Sciences, LLC as a deoxyribonucleoside phosphoramidite. All other bases were purchased from Glen Research. Nucleosides were incorporated during the appropriate cycle on a 0.2 μmol scale; see Table S7 for sequences. Upon completion of the synthesis, columns were evaporated under reduced pressure for 4 h. Deprotection of dZ containing oligos was initiated by treating the solid support with 1 M 1,8-diazabicyclo[5.4.0]undec-7-ene in acetonitrile at room temperature for 10 h. After 10 h, the mixture was centrifuged at 13 200 × g for 5 min. The supernatant was discarded, and the support was dried under reduced pressure before proceeding with cleavage. All oligonucleotides were cleaved from the solid support by treatment with 1:3 ethanol/30% NH_4OH at 55 °C for 12 h. The supernatant was transferred to a new screw-cap tube and evaporated under reduced pressure. Desilylation was performed by resuspending the pellets in anhydrous DMSO and treating with 55% (v/v) Et_3N-3HF at room temperature overnight. To each reaction was added 75 mM sodium acetate in butanol. The oligonucleotides were then precipitated from a solution of 65% butanol at −70 °C for 2 h. The solution was centrifuged at 13 200 × g for 20 min, supernatant was removed, and the pellet was washed twice with cold 95% ethanol. The RNA pellets were then desalted using a Sephadex G-25 column and purified as described below.

Purification of Oligonucleotides.

Single-stranded RNA oligonucleotides were purified by denaturing polyacrylamide gel electrophoresis and visualized by UV shadowing. Bands were excised from the gel, crushed, and soaked overnight at 4 °C in 0.5 M NaOAc, 0.1% sodium dodecyl sulfate (SDS), and

0.1 mM EDTA. Polyacrylamide fragments were removed with a 0.2 μm filter, and the RNAs were precipitated from a solution of 75% EtOH at −70 °C for 4 h. The solution was centrifuged 13 200 × g for 20 min, and supernatant was removed. The RNA solutions were lyophilized to dryness, resuspended in nuclease-free water, and quantified by absorbance at 260 nm. dZ and 8-azanebularine containing oligonucleotides used for crystallography were additionally desalted by four rounds of concentration and subsequent addition of nuclease-free water in a 3000 NMWL Amicon Ultra 0.5 mL centrifugal filter. Oligonucleotide mass was confirmed by MALDI-TOF.

In Vitro Transcription of Editing Target RNA.

Target RNA was transcribed from a DNA template with the MEGAScript T7 Kit (ThermoFisher). DNA Digestion was performed using RQ1 RNase-free DNase (Promega). DNase treated RNA product was purified as described above.

Preparation of Duplex Substrates for Analysis of ADAR Deamination Kinetics.

Purified guide and transcribed RNA were added in a 10:1 ratio to hybridization buffer (180 nM transcribed RNA target, 1.8 μM guide, 1X TE Buffer, 100 mM NaCl), heated to 95 °C for 5 min, and slowly cooled to room temperature.

Preparation of Duplex Substrates for Crystallography.

dZ and 8-azanebularine containing oligonucleotides were hybridized in a 1:1 ratio in nuclease-free water by heating the mixture to 95 °C for 5 min and slow cooling to room temperature.

Protein Overexpression and Purification of ADAR2 Full Length Constructs.

hADAR2 wild-type (hADAR2 WT) was expressed and as previously described.[54] Purification of hADAR2 was carried out by lysing cells in buffer containing 20 mM Tris-HCl, pH 8.0, 5% glycerol, 1 mM BME, 750 mM NaCl, 35 mM imidazole, and 0.01% Nonidet P-40 using a French press. Cell lysate was clarified by centrifugation (44 000 × g for 1 h). Lysate was passed over a 3 mL Ni-NTA column, which was then washed in three steps with 20 mL of lysis buffer, wash I buffer (20 mM Tris-HCl, pH 8.0, 5% glycerol, 1 mM BME, 750 mM NaCl, 35 mM imidazole, 0.01% Nonidet P-40), and wash II buffer (20 mM Tris-HCl, pH 8.0, 5% glycerol, 1 mM BME, 35 mM imidazole, 500 mM NaCl), and eluted with 20 mM Tris-HCl, pH 8.0, 5% glycerol, 1 mM BME, 400 mM imidazole, and 100 mM NaCl. Fractions containing the target protein were pooled and concentrated to 30–80 μM for use in biochemical assays. Protein concentrations were determined using BSA standards visualized by SYPRO orange staining of SDS-polyacrylamide gels. Purified hADAR2 WT was stored in 20 mM Tris-HCl pH 8.0, 100 mM NaCl, 20% glycerol, and 1 mM BME at −70 °C.

Protein Overexpression and Purification of ADAR1 p110.

MBP-tagged human ADAR1 p110 wild-type (hADAR1 p110 WT) was expressed as previously described.[24] Purification of hADAR1 p110 was carried out by lysing cells in buffer containing 50 mM Tris-HCl, pH 8.0, 5% glycerol, 5 mM BME, 1000 mM KCl,

50 μM $ZnCl_2$, and 0.05% NP-40 using a microfluidizer. Cell lysate was clarified by centrifugation (39 000 × g for 50 min). Lysate was passed over a 2 mL NEB amylose column, which was then washed in two steps with 50 mL of lysis buffer and 100 mL of wash I buffer (50 mM Tris-HCl, pH 8.0, 5% glycerol, 5 mM BME, 500 mM KCl, 50 μM $ZnCl_2$, 0.01% Nonidet P-40) and eluted with 50 mM Tris-HCl, pH 8.0, 10% glycerol, 5 mM BME, 500 mM KCl, 50 μM $ZnCl_2$, 0.01% Nonidet P-40, and 20 mM maltose. Fractions containing the target protein were pooled and concentrated to 5–50 μM for use in biochemical assays. Protein concentrations were determined using BSA standards visualized by SYPRO orange staining of SDS-polyacrylamide gels. Purified hADAR1 p110 WT was stored in 50 mM Tris-HCl pH 8.0, 400 mM KCl, 0.5 mM EDTA, 0.01% NP-40, 10% glycerol, and 1 mM tris(2-carboxyethyl)phosphine at −70 °C.

In Vitro Deamination Kinetics.

Deamination assays were performed under single-turnover conditions. Reactions with ADAR2 wild-type (WT) or E488Q contained 15 mM Tris-HCl pH 7.5, 3% glycerol, 60 mM KCl, 1.5 mM EDTA, 0.003% Nonidet P-40, 3 mM $MgCl_2$, 160 U/mL RNAsin, 1.0 μg/mL, 0.8 nM RNA, and 2 nM enzyme. ADAR1 reactions contained 15 mM Tris-HCl pH 7.5, 4% glycerol, 26 mM KCl, 40 mM potassium glutamate, 1.5 mM EDTA, 0.003% Nonidet P-40, 160 U/mL RNAsin, 1.0 μg/mL yeast tRNA, 5 nM RNA, and 50 nM ADAR1 p110 wild-type. Each reaction solution was incubated at 30 °C for 30 min before adding enzyme and allowed to incubate at 30 °C for varying times prior to stopping with 190 μL of 95 °C water and heating at 95 °C for 5 min. RT-PCR (Promega Access RT-PCR System) was used to generate cDNA from deaminated RNA. The resulting cDNA was purified using the DNA Clean & Concentrator kit from Zymo and subjected to Sanger Sequencing using an ABI Prism 3730 Genetic Analyzer at the UC Davis DNA Sequencing Facility with the forward PCR primers. The sequencing peak heights were quantified in 4Peaks v1.8. Each experiment was carried out in triplicate. The editing level for the corresponding zero time point was subtracted from each data point as a background subtraction.

Preparation of Duplex Substrates for Base Flipping Analysis.

PAGE purified top and bottom strands were annealed for a final concentration of 30 μM edited strand, 45 μM guide strand, 30 mM Tris-HCl, 6% glycerol, 120 mM KCl, 3 mM EDTA, 0.006% NP-40, and 0.6 mM DTT. The mixture was heated to 95 °C for 5 min and slowly cooled to room temperature.

Plate-Based Assay Using a Fluorescent RNA Substrate to Monitor Base Flipping by ADAR2.

Fluorescence measurements were performed using a CLARIOstar microplate reader and a 384-well black bottom plate. Excitation was at 320 nm, and fluorescence emission was scanned from 340 to 430 nm. Spectra were obtained for solutions containing 2.5 μM RNA, with or without 10 μM ADAR2, in 36 mM Tris-HCl at pH 7.5, 7% glycerol, 142 mM KCl, 3.6 mM EDTA, 0.007% NP-40, and 0.7 mM DTT at room temperature. The background fluorescence of the enzyme solution was subtracted from the spectrum of the complex, and the background fluorescence of the buffer alone was subtracted from the RNA.

Expression and Purification of hADAR2 Deaminase Domain (hADAR2d) for Crystallography.

Protein expression and purification was carried out according to previously reported protocols.[20] In short, BCY123 yeast cells were transformed with a pSc-ADAR plasmid encoding hADAR2d-WT using a high lithium transformation. Cells were plated on yeast minimal media minus uracil plates (CM-Ura+Glucose). An isolated colony was used to inoculate 15 mL of CM-Ura+Glucose media and incubated at 30 °C with shaking at 300 rpm overnight. A 1 L volume of CM-Ura+Glycerol/Lactate yeast growth media was inoculated with 12 mL of starter culture. After 24 h, cells were induced by adding 110 mL of sterile 30% galactose solution per liter of culture and protein was expressed for 6 h. Cells were collected by centrifugation at 5000 × *g* for 15 min, and cell pellets were stored at −80 °C until purification. A cell pellet corresponding to a 2 L growth was resuspended in cold Buffer A (20 mM Tris-HCl pH 8.0, 5% glycerol, 35 mM imidazole, 0.01% Triton × 100, 1 mM β-mercaptoethanol) with 750 mM NaCl. Cells were lysed on a microfluidizer and lysate clarified by centrifugation at 39 000 × *g* for 45 min. Lysate was filtered through 0.45 μm filter and passed over a 1 mL Ni-NTA column and washed with 20 mL of Buffer A + 750 mM NaCl. Loaded Ni-NTA resin was then washed with 60 mL of Wash Buffer I (Buffer A + 400 mM NaCl) followed by 30 mL of Wash Buffer II (Buffer A + 100 mM NaCl). Target protein was eluted with a 35–300 mM imidazole elution gradient in Wash Buffer II over 60 min at a flow rate of 1 mL/min. Fractions were analyzed on SDS-PAGE, and fractions containing the target protein were pooled and loaded onto a 1 mL GE Healthcare Lifesciences Hi-Trap Heparin HP column at a flow rate of 0.5 mL/min. The loaded heparin resin was washed with 30 mL of Wash Buffer II (Buffer A + 100 mM NaCl), and target protein was eluted with a gradient of 100–1000 mM NaCl in Wash Buffer II (Buffer A + 100 mM NaCl) over 30 min at a flow rate of 1 mL/min. Fractions containing the target protein were pooled, and the 10xHis tag was cleaved with a 1:1 mass ratio of TEV to target protein for 2 h at room temperature. The cleaved protein was collected by passing the cleavage reaction over another Ni-NTA column at a flow rate of 0.5 mL/min. The flowthrough and wash were collected and dialyzed against SEC Buffer (20 mM Tris pH 8.0, 200 mM NaCl, 5% glycerol, and 1 mM β-mercaptoethanol). Dialyzed protein was then concentrated to 500 μL using an Amicon Ultra centrifugation filter with a 30 000 NMWL. Concentrated protein was loaded onto a GE Healthcare HiLoad 16/600 Superdex PG column equilibrated with SEC Buffer. Fractions containing purified protein were pooled and concentrated for crystallography trials using centrifugal filtration.

hADAR2d-*GLI1*-dZ Complex Crystallization.

Crystals of the human ADAR2 deaminase domain WT (hADAR2d WT)/dZ complex were grown at room temperature using the sitting-drop vapor diffusion method. A 1 μL solution of 4.5 mg/mL hADAR2d WT and 100 μM of *GLI1*-dZ 23mer RNA (1:1 hADAR2d WT:RNA molar ratio) were mixed with 1 μL of 0.1 M MES:NaOH pH 6.5 and 10% PEG 20,000. Crystals appeared within 2 weeks as a cluster of plates. A single crystal was broken off the cluster, soaked in a solution of mother liquor and 30% glycerol, and flash-cooled in liquid nitrogen. Data were collected via fine-phi slicing using 0.2° oscillations at beamline 24-ID-E at the Advanced Photon Source at Argonne National Laboratory. X-ray diffraction data were collected to 2.50 Å resolution.

Processing and Refinement of Crystallographic Data.

Crystallographic data were processed using XDS[55] and scaled using Aimless (CCP4 1994).[56] The structure of a hADAR2d mutant E488Y bound to dsRNA (PDB ID: 6D06)[42] was used as a phasing model for molecular replacement using PHENIX.[57] The structure was refined using PHENIX[58] including TLS parameters, simulated annealing, and Zn coordinate restraints. The model was built and adjusted using COOT.[59] Ideal Zn–ligand distances were determined using average distances found in previously deposited ADAR structures and in the MetalPDB database.[60] As indicated by the Matthews coefficient (CCP4),[61] molecular replacement successfully placed two protein monomers one of which was bound to dsRNA as observed in previous structures.[44] In each protein monomer (chains A and D), the C-terminal proline (Pro701) was disordered and thus not included in the model. Geometry restraints from previous hADAR2d-dsRNA structures were used to model in the hydrated 8-azanebularine.[20] Geometry restraints for the dZ base were calculated by Monomer Library Sketcher (CCP4).[56] The structure refined to a final R_{factor} and R_{free} of 17.30% and 22.60%, respectively. Table S4 shows the data processing and model refinement statistics. Atomic coordinates and structure factors have been deposited to the Protein Data Bank (PDB ID: 7KFN)

Density Functional Theory Calculations of Benner's Base Z and Cytosine.

Structures of Benner's Base Z and cytosine were fully optimized using the M06–2X/6–311+G(2d,p) method[62] as implemented in GAUSSIAN16.[63] Frequency analysis confirmed the structures to be minima. Partial charges were computed using the CHelpG model.[64]

Directed Editing on the Endogenous *RAB7A* Target in HEK293T Cells.

HEK293T cells were cultured in Dulbecco's Modified Eagle Medium (DMEM) (Gibco, 11995–065) with 10% fetal bovine serum (FBS) (Thermo Fisher, 26140–087) and additionally supplemented with 1X antibiotic-antimycotic (Thermo Fisher, 15240–062) at 37 °C, 5% CO_2. Once cells reached 70–90% confluency, cells were seeded into 96 well plates (6.4×10^3 cells per well). After 24 h, cells were cotransfected with 500 ng of ADAR plasmid and 50 nM guide oligonucleotide using Lipofectamine 2000 (Thermo Fisher, 11668–019). After incubation of transfection reagent, plasmid, and guide oligonucleotide in Opti-MEM Reduced Serum Media (Thermo Fisher, 31985–062), the solution was added to designated wells and incubated at 37 °C, 5% CO_2. After 48 h, total RNA was isolated using RNAqueous Total RNA Isolation Kit (Thermo Fisher, AM1912) and DNase treated with RQ1 RNase-free DNase (Promega, M6101). Nested RT-PCR was performed in triplicate using Access RT-PCR kit (Promega, A1280) for 20 cycles and then followed by Phusion Hot Start II DNA Polymerase (Thermo Fisher, F-549L) for the second PCR of 30 cycles with target specific primers (Table S7). PCR product was purified by agarose gel and QIAquick Gel Extraction kit (Qiagen, 28706). Product was submitted for Sanger Sequencing, and sequence traces were analyzed by 4Peaks (Nucleobytes) to quantify percent editing.

Directed Editing on the Endogenous WT *APP* Target in Human Retinal Pigment Epithelium Cells (ARPE-19).

Spontaneously arising human retinal pigment epithelium cell line (ARPE-19) carrying the wild-type *APP* gene was obtained from ATCC (ATCC CRL-2302, Lot. 70013110). Briefly, 1.5×10^5 ARPE-19 cells per well were seeded in a 12-well plate 24 h before transfection. Transfection was performed with 100 nM guide strand and Lipofectamine 2000 (Invitrogen) according to the manufacturer's instructions (at a ratio of 1:2, 1 μg of guide strand to 2 μL of Lipofectamine 2000). A nontransfection (NT), a mock transfection, and a scrambled guide strand (Table S7) were used as negative controls. Total RNA was extracted from cells 48 h after transfection using the Direct-zol RNA MicroPrep (Zymo Research) kit according to the manufacturer's instructions, and ~500 ng of total RNA were used to prepare cDNA using the Maxima reverse transcriptase kit (Thermo Fisher) according to the manufacturer's instructions, with a combination of random hexamer and oligo-dT primers. Digital droplet PCR (ddPCR) was performed using 1 μL of a 10× dilution of cDNA. The ddPCR assay for absolute quantification of nucleic acid target sequences was performed using BioRad's QX-200 Droplet Digital PCR system. Diluted cDNA obtained from RT-PCR was used in a total mixture of 21 μL of reaction mix, including the ddPCR Supermix for Probes no dUTP (Bio Rad), a Taqman SNP genotype assay with forward and reverse primers combined with the gene-specific probes (Table S7). The PCR mix was filled in the middle row of a ddPCR cartridge (BioRad) using a multichannel pipet. The replicates were divided by two cartridges. The bottom rows were filled with 70 μL of droplet generation oil for probes (BioRad). After the rubber gasket replacement, droplets were generated in the QX200 droplet generator. An oil emulsion volume of 42 μL from the top row of the cartridge was transferred to a 96-well PCR plate. The PCR plate was sealed with tin foil for 4 s at 170 °C using the PX1 plate sealer, followed by the following PCR program: 1 cycle of enzyme activation for 10 min at 95 °C, 40 cycles of denaturation for 30 s at 95 °C and annealing/extension for 1 min at 53.8 °C, 1 cycle of enzyme deactivation for 10 min at 98 °C, followed by storage at 8 °C. After PCR, the plate was read and analyzed with the QX200 droplet reader.

Directed Editing on the Endogenous *Idua* Target in Mouse Primary Liver Fibroblasts.

Homozygous *Idua-W392X* mice on a C57BL/6 background were obtained under a license agreement from the UAB Research Foundation (UABRF). Mouse primary liver fibroblasts were isolated from homozygous *Idua-W392X* mice using a Liver Dissociation kit, mouse (Miltenyi Biotech, 130-105-807). Cells were seeded with 3.0×10^5 cells per well in a collagen coated 6-well plate 24 h prior to transfection. Transfection, RNA extraction, and analysis were carried out using the protocol described above, with the following changes: Direct-zol RNA MiniPrep Kit (Zymo Research) was used for RNA extraction, 1 μL of a 3× dilution of cDNA was used as a template for ddPCR, and the annealing/extension step of ddPCR was caried out at 63.8 °C.

Supplementary Material

Refer to Web version on PubMed Central for supplementary material.

ACKNOWLEDGMENTS

E.E.D. was supported by a training grant [GM113770] from the National Institutes of Health. The content of this publication is solely the responsibility of the authors and do not necessarily represent the official views of the NIH. A.J.F. is partially supported by the United States Department of Agriculture National Institute of Food and Agriculture Hatch Grant [CA-D-MCB-2629-H] and by the University of California Cancer Research Coordinating Committee [CRR-20-637188]. This work is based upon research conducted at the Northeastern Collaborative Access Team beamlines, which are funded by the National Institute of General Medical Sciences from the National Institutes of Health [P30 GM124165]. The Eiger 16M detector on the 24-ID-E beamline is funded by an NIH-ORIP HEI grant [S10OD021527]. This research used resources of the Advanced Photon Source, a U.S. Department of Energy (DOE) Office of Science User Facility operated for the DOE Office of Science by Argonne National Laboratory under Contract No. DE-AC02-06CH11357. We would like to thank the University of California, Davis DNA Sequencing Facility and the University of California Davis Campus Mass Spectrometry Facilities Core.

Data Availability:

Atomic coordinates and structure factors have been deposited in the Protein Data Bank under the accession code 7KFN.

REFERENCES

(1). Villiger L; Grisch-Chan HM; Lindsay H; Ringnalda F; Pogliano CB; Allegri G; Fingerhut R; Häberle J; Matos J; Robinson MD; Thöny B; Schwank G Treatment of a Metabolic Liver Disease by in Vivo Genome Base Editing in Adult Mice. Nat. Med 2018, 24 (10), 1519–1525. [PubMed: 30297904]

(2). Sinnamon JR; Kim SY; Corson GM; Song Z; Nakai H; Adelman JP; Mandel G Site-Directed RNA Repair of Endogenous Mecp2 RNA in Neurons. Proc. Natl. Acad. Sci. U. S. A 2017, 114 (44), E9395–E9402. [PubMed: 29078406]

(3). Yeh W-H; Chiang H; Rees HA; Edge ASB; Liu DR In Vivo Base Editing of Post-Mitotic Sensory Cells. Nat. Commun 2018, 9 (1), 2184. [PubMed: 29872041]

(4). Bass BL RNA Editing by Adenosine Deaminases That Act on RNA. Annu. Rev. Biochem 2002, 71 (I), 817–846. [PubMed: 12045112]

(5). Zhao X; Yu Y-T Targeted Pre-MRNA Modification for Gene Silencing and Regulation. Nat. Methods 2008, 5 (1), 95–100. [PubMed: 18066073]

(6). Karijolich J; Yu Y-T Converting Nonsense Codons into Sense Codons by Targeted Pseudouridylation. Nature 2011, 474 (7351), 395–398. [PubMed: 21677757]

(7). Fire A; Xu S; Montgomery MK; Kostas SA; Driver SE; Mello CC Potent and Specific Genetic Interference by Double-Stranded RNA in Caenorhabditis Elegans. Nature 1998, 391 (6669), 806–811. [PubMed: 9486653]

(8). Jinek M; Chylinski K; Fonfara I; Hauer M; Doudna JA; Charpentier E A Programmable Dual-RNA–Guided DNA Endonuclease in Adaptive Bacterial Immunity. Science (Washington, DC, U. S.) 2012, 337 (6096), 816–821.

(9). Qu L; Yi Z; Zhu S; Wang C; Cao Z; Zhou Z; Yuan P; Yu Y; Tian F; Liu Z; Bao Y; Zhao Y; Wei W Programmable RNA Editing by Recruiting Endogenous ADAR Using Engineered RNAs. Nat. Biotechnol 2019, 37 (9), 1059–1069. [PubMed: 31308540]

(10). Wilbie D; Walther J; Mastrobattista E Delivery Aspects of CRISPR/Cas for in Vivo Genome Editing. Acc. Chem. Res 2019, 52 (6), 1555–1564. [PubMed: 31099553]

(11). Colella P; Ronzitti G; Mingozzi F Emerging Issues in AAV-Mediated *In Vivo* Gene Therapy. Mol. Ther.–Methods Clin. Dev 2018, 8, 87–104. [PubMed: 29326962]

(12). Crudele JM; Chamberlain JS Cas9 Immunity Creates Challenges for CRISPR Gene Editing Therapies. Nat. Commun 2018, 9 (1), 3497. [PubMed: 30158648]

(13). Merkle T; Merz S; Reautschnig P; Blaha A; Li Q; Vogel P; Wettengel J; Li JB; Stafforst T Precise RNA Editing by Recruiting Endogenous ADARs with Antisense Oligonucleotides. Nat. Biotechnol 2019, 37 (2), 133–138. [PubMed: 30692694]

(14). Katrekar D; Chen G; Meluzzi D; Ganesh A; Worlikar A; Shih Y-R; Varghese S; Mali P In Vivo RNA Editing of Point Mutations via RNA-Guided Adenosine Deaminases. Nat. Methods 2019, 16 (3), 239–242. [PubMed: 30737497]

(15). Stafforst T; Schneider MF An RNA–Deaminase Conjugate Selectively Repairs Point Mutations. Angew. Chem., Int. Ed 2012, 51 (44), 11166–11169.

(16). Montiel-Gonzalez MF; Vallecillo-Viejo I; Yudowski GA; Rosenthal JJCC Correction of Mutations within the Cystic Fibrosis Transmembrane Conductance Regulator by Site-Directed RNA Editing. Proc. Natl. Acad. Sci. U. S. A 2013, 110 (45), 18285–18290. [PubMed: 24108353]

(17). Azad MTAA; Bhakta S; Tsukahara T Site-Directed RNA Editing by Adenosine Deaminase Acting on RNA for Correction of the Genetic Code in Gene Therapy. Gene Ther. 2017, 24 (12), 779–786. [PubMed: 28984845]

(18). Cox DBTT; Gootenberg JS; Abudayyeh OO; Franklin B; Kellner MJ; Joung J; Zhang F RNA Editing with CRISPR-Cas13. Science (Washington, DC, U. S.) 2017, 358 (6366), 1019–1027.

(19). Chen G; Katrekar D; Mali P RNA-Guided Adenosine Deaminases: Advances and Challenges for Therapeutic RNA Editing. Biochemistry 2019, 58 (15), 1947–1957. [PubMed: 30943016]

(20). Matthews MM; Thomas JM; Zheng Y; Tran K; Phelps KJ; Scott AI; Havel J; Fisher AJ; Beal PA Structures of Human ADAR2 Bound to DsRNA Reveal Base-Flipping Mechanism and Basis for Site Selectivity. Nat. Struct. Mol. Biol 2016, 23 (5), 426–433. [PubMed: 27065196]

(21). Lehmann KA; Bass BL Double-Stranded RNA Adenosine Deaminases ADAR1 and ADAR2 Have Overlapping Specificities. Biochemistry 2000, 39 (42), 12875–12884. [PubMed: 11041852]

(22). Wong SK; Sato S; Lazinski DW Substrate Recognition by ADAR1 and ADAR2. RNA 2001, 7 (6), 846–858. [PubMed: 11421361]

(23). Kuttan A; Bass BL Mechanistic Insights into Editing-Site Specificity of ADARs. Proc. Natl. Acad. Sci. U. S. A 2012, 109 (48), E3295–E3304. [PubMed: 23129636]

(24). Malik TN; Doherty EE; Gaded VM; Hill TM; Beal PA; Emeson RB Regulation of RNA Editing by Intracellular Acidification. Nucleic Acids Res. 2021, 49, 4020–4036. [PubMed: 33721028]

(25). Chin T-M; Lin S-B; Lee S-Y; Chang M-L; Cheng AY-Y; Chang F-C; Pasternack L; Huang D-H; Kan L-S Paper-Clip" Type Triple Helix Formation by 5'-d-(TC)3Ta(CT)3Cb(AG)3 (a and b = 0–4) as a Function of Loop Size with and without the Pseudoisocytosine Base in the Hoogsteen Strand. Biochemistry 2000, 39 (40), 12457–12464. [PubMed: 11015227]

(26). Burchenal JH; Ciovacco K; Kalaher K; O'Toole T; Kiefner R; Dowling MD; Chu CK; Watanabe KA; Wempen I; Fox JJ Antileukemic Effects of Pseudoisocytidine, a New Synthetic Pyrimidine C-Nucleoside. Cancer Res. 1976, 36 (4), 1520–1523. [PubMed: 1260769]

(27). Lu J; Li N-S; Koo SC; Piccirilli JA Synthesis of Pyridine, Pyrimidine and Pyridinone C-Nucleoside Phosphoramidites for Probing Cytosine Function in RNA. J. Org. Chem 2009, 74 (21), 8021–8030. [PubMed: 19791761]

(28). Yang Z; Hutter D; Sheng P; Sismour AM; Benner SA Artificially Expanded Genetic Information System: A New Base Pair with an Alternative Hydrogen Bonding Pattern. Nucleic Acids Res. 2006, 34 (21), 6095–6101. [PubMed: 17074747]

(29). Cho IS; Kim J; Lim DH; Ahn H-C; Kim H; Lee K-B; Lee YS Improved Serum Stability and Biophysical Properties of SiRNAs Following Chemical Modifications. Biotechnol. Lett 2008, 30 (11), 1901. [PubMed: 18575806]

(30). Kratschmer C; Levy M Effect of Chemical Modifications on Aptamer Stability in Serum. Nucleic Acid Ther. 2017, 27 (6), 335–344. [PubMed: 28945147]

(31). Stephens OM; Yi-Brunozzi HY; Beal PA Analysis of the RNA-Editing Reaction of ADAR2 with Structural and Fluorescent Analogues of the GluR-B R/G Editing Site. Biochemistry 2000, 39 (40), 12243–12251. [PubMed: 11015203]

(32). Holz B; Weinhold E; Klimasauskas S; Serva S 2-Aminopurine as a Fluorescent Probe for DNA Base Flipping by Methyltransferases. Nucleic Acids Res. 1998, 26 (4), 1076–1083. [PubMed: 9461471]

(33). Jeltsch A; Roth M; Friedrich T Mutational Analysis of Target Base Flipping by the EcoRV Adenine-N6 DNA Methyltransferase. J. Mol. Biol 1999, 285 (3), 1121–1130. [PubMed: 9918720]

(34). Hartono YD; Pabon-Martinez YV; Uyar A; Wengel J; Lundin KE; Zain R; Smith CIE; Nilsson L; Villa A Role of Pseudoisocytidine Tautomerization in Triplex-Forming Oligonucleotides: In Silico and in Vitro Studies. ACS Omega 2017, 2 (5), 2165–2177. [PubMed: 30023656]

(35). Wang D; Shukla C; Liu X; Schoeb TR; Clarke LA; Bedwell DM; Keeling KM Characterization of an MPS I-H Knock-in Mouse That Carries a Nonsense Mutation Analogous to the Human IDUA-W402X Mutation. Mol. Genet. Metab 2010, 99 (1), 62–71. [PubMed: 19751987]

(36). Scott HS; Litjens T; Nelson PV; Thompson PR; Brooks DA; Hopwood JJ; Morris CP Identification of Mutations in the Alpha-L-Iduronidase Gene (IDUA) That Cause Hurler and Scheie Syndromes. Am. J. Hum. Genet 1993, 53 (5), 973–986. [PubMed: 8213840]

(37). Guschlbauer W; Duplaa AM; Guy A; Téoule R; Fazakerley GV Structure and in Vitro Replication of DNA Templates Containing 7,8-Dihydro-8-Oxoadenine. Nucleic Acids Res. 1991, 19 (8), 1753–1758. [PubMed: 1851559]

(38). Park SH; Doherty EE; Xie Y; Padyana AK; Fang F; Zhang Y; Karki A; Lebrilla CB; Siegel JB; Beal PA High-Throughput Mutagenesis Reveals Unique Structural Features of Human ADAR1. Nat. Commun 2020, 11 (1), 5130. [PubMed: 33046702]

(39). Wang Y; Havel J; Beal PA A Phenotypic Screen for Functional Mutants of Human Adenosine Deaminase Acting on RNA 1. ACS Chem. Biol 2015, 10 (11), 2512–2519. [PubMed: 26372505]

(40). Montiel-González MF; Vallecillo-Viejo IC; Rosenthal JJC An Efficient System for Selectively Altering Genetic Information within MRNAs. Nucleic Acids Res. 2016, 44 (21), e157–e157. [PubMed: 27557710]

(41). Vallecillo-Viejo IC; Liscovitch-Brauer N; Montiel-Gonzalez MF; Eisenberg E; Rosenthal JJCC Abundant Off-Target Edits from Site-Directed RNA Editing Can Be Reduced by Nuclear Localization of the Editing Enzyme. RNA Biol. 2018, 15 (1), 104–114. [PubMed: 29099293]

(42). Monteleone LR; Matthews MM; Palumbo CM; Thomas JM; Zheng Y; Chiang Y; Fisher AJ; Beal PA A Bump-Hole Approach for Directed RNA Editing. Cell Chem. Biol 2019, 26 (2), 269–277.e5. [PubMed: 30581135]

(43). Haudenschild BL; Maydanovych O; Véliz EA; Macbeth MR; Bass BL; Beal PA A Transition State Analogue for an RNA-Editing Reaction. J. Am. Chem. Soc 2004, 126 (36), 11213–11219. [PubMed: 15355102]

(44). Thuy-Boun AS; Thomas JM; Grajo HL; Palumbo CM; Park SH; Nguyen LT; Fisher AJ; Beal PA Asymmetric Dimerization of Adenosine Deaminase Acting on RNA Facilitates Substrate Recognition. Nucleic Acids Res. 2020, 48 (14), 7958–7972. [PubMed: 32597966]

(45). Wettengel J; Reautschnig P; Geisler S; Kahle PJ; Stafforst T Harnessing Human ADAR2 for RNA Repair – Recoding a PINK1Mutation Rescues Mitophagy. Nucleic Acids Res. 2016, 45 (5), 2797–2808.

(46). Li JB; Levanon EY; Yoon J-K; Aach J; Xie B; LeProust E; Zhang K; Gao Y; Church GM Genome-Wide Identification of Human RNA Editing Sites by Parallel DNA Capturing and Sequencing. Science (Washington, DC, U. S.) 2009, 324 (5931), 1210–1213.

(47). Schneider MF; Wettengel J; Hoffmann PC; Stafforst T Optimal GuideRNAs for Re-Directing Deaminase Activity of HADAR1 and HADAR2 in Trans. Nucleic Acids Res. 2014, 42 (10), e87–e87. [PubMed: 24744243]

(48). Vogel P; Moschref M; Li Q; Merkle T; Selvasaravanan KD; Li JB; Stafforst T Efficient and Precise Editing of Endogenous Transcripts with SNAP-Tagged ADARs. Nat. Methods 2018, 15 (7), 535–538. [PubMed: 29967493]

(49). Vogel P; Schneider MF; Wettengel J; Stafforst T Improving Site-Directed RNA Editing In Vitro and in Cell Culture by Chemical Modification of the GuideRNA. Angew. Chem., Int. Ed 2014, 53 (24), 6267–6271.

(50). Woolf TM; Chase JM Stinchcomb, D. T. Toward the Therapeutic Editing of Mutated RNA Sequences. Proc. Natl. Acad. Sci. U. S. A 1995, 92 (18), 8298–8302. [PubMed: 7545300]

(51). Schaffer AA; Kopel E; Hendel A; Picardi E; Levanon EY; Eisenberg E The Cell Line A-to-I RNA Editing Catalogue. Nucleic Acids Res. 2020, 48 (11), 5849–5858. [PubMed: 32383740]

(52). Heep M; Mach P; Reautschnig P; Wettengel J; Stafforst T Applying Human ADAR1p110 and ADAR1p150 for Site-Directed RNA Editing-G/C Substitution Stabilizes GuideRNAs against Editing. Genes 2017, 8 (1), 34.

(53). Prakash TP; Graham MJ; Yu J; Carty R; Low A; Chappell A; Schmidt K; Zhao C; Aghajan M; Murray HF; Riney S; Booten SL; Murray SF; Gaus H; Crosby J; Lima WF; Guo S; Monia BP; Swayze EE; Seth PP Targeted Delivery of Antisense Oligonucleotides to Hepatocytes Using Triantennary N-Acetyl Galactosamine Improves Potency 10-Fold in Mice. Nucleic Acids Res. 2014, 42 (13), 8796–8807. [PubMed: 24992960]

(54). Macbeth MR; Bass BL Large-Scale Overexpression and Purification of ADARs from Saccharomyces Cerevisiae for Biophysical and Biochemical Studies. Methods Enzymol. 2007, 424, 319–331. [PubMed: 17662848]

(55). Kabsch W XDS. Acta Crystallogr., Sect. D: Biol. Crystallogr 2010, 66 (2), 125–132. [PubMed: 20124692]

(56). Winn MD; Ballard CC; Cowtan KD; Dodson EJ; Emsley P; Evans PR; Keegan RM; Krissinel EB; Leslie AGW; McCoy A; McNicholas SJ; Murshudov GN; Pannu NS; Potterton EA; Powell HR; Read RJ; Vagin A; Wilson KS Overview of the CCP4 Suite and Current Developments. Acta Crystallogr., Sect. D: Biol. Crystallogr 2011, 67 (4), 235–242. [PubMed: 21460441]

(57). McCoy AJ; Grosse-Kunstleve RW; Adams PD; Winn MD; Storoni LC; Read RJ Phaser Crystallographic Software. J. Appl. Crystallogr 2007, 40 (4), 658–674. [PubMed: 19461840]

(58). Afonine PV; Grosse-Kunstleve RW; Echols N; Headd JJ; Moriarty NW; Mustyakimov M; Terwilliger TC; Urzhumtsev A; Zwart PH; Adams PD Towards Automated Crystallographic Structure Refinement with {\it Phenix.Refine}. Acta Crystallogr., Sect. D: Biol. Crystallogr 2012, 68 (4), 352–367. [PubMed: 22505256]

(59). Emsley P; Cowtan K Coot: Model-Building Tools for Molecular Graphics. Acta Crystallogr., Sect. D: Biol. Crystallogr 2004, 60 (12), 2126–2132. [PubMed: 15572765]

(60). Putignano V; Rosato A; Banci L; Andreini C MetalPDB in 2018: A Database of Metal Sites in Biological Macromolecular Structures. Nucleic Acids Res. 2018, 46 (D1), D459–D464. [PubMed: 29077942]

(61). Matthews BW Solvent Content of Protein Crystals. J. Mol. Biol 1968, 33 (2), 491–497. [PubMed: 5700707]

(62). Zhao Y; Truhlar DG The M06 Suite of Density Functionals for Main Group Thermochemistry, Thermochemical Kinetics, Noncovalent Interactions, Excited States, and Transition Elements: Two New Functionals and Systematic Testing of Four M06-Class Functionals and 12 Other Function. Theor. Chem. Acc 2008, 120 (1), 215–241.

(63). Frisch MJ; Trucks GW; Schlegel HB; Scuseria GE; Robb MA; Cheeseman JR; Scalmani G; Barone V; Petersson GA Gaussian 16, Rev. C.01; Gaussian, Inc.: 2016.

(64). Breneman CM; Wiberg KB Determining Atom-centered Monopoles from Molecular Electrostatic Potentials. The Need for High Sampling Density in Formamide Conformational Analysis. J. Comput. Chem 1990, 11, 361.

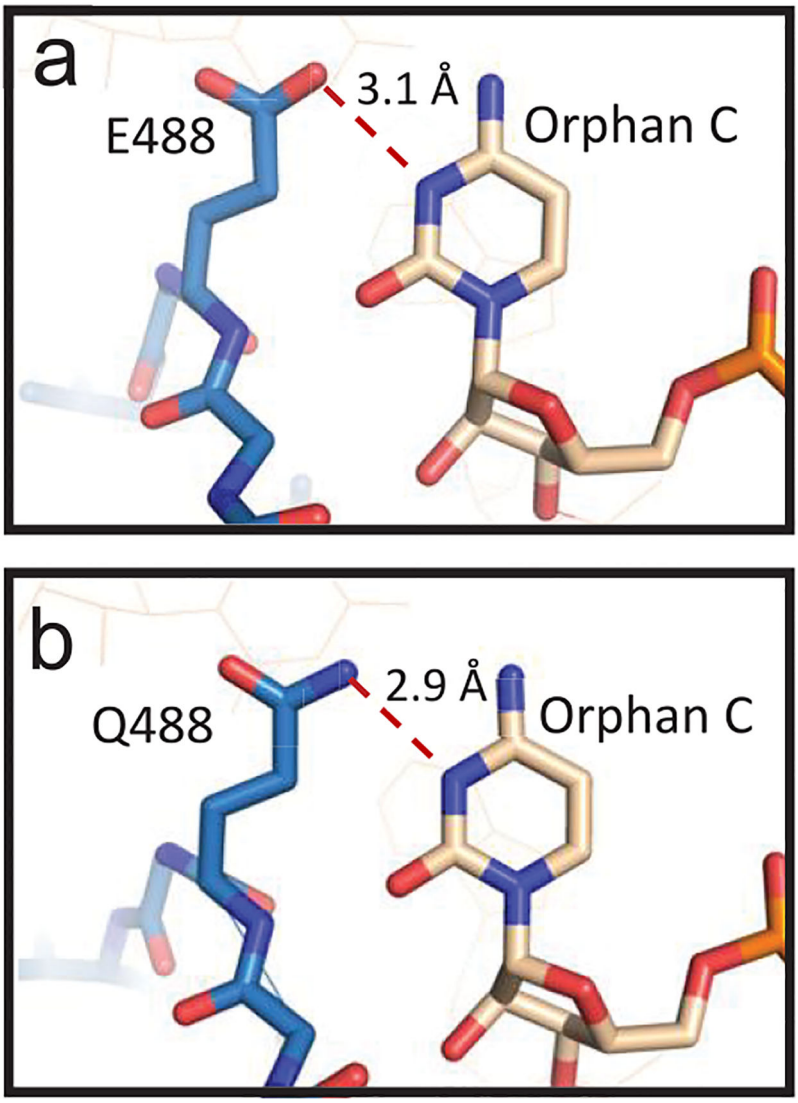

Figure 1.

(a) The intercalating E488 residue of the ADAR2 flipping loop is engaged in a suspected hydrogen-bonding interaction with N3 of the orphan cytidine (PDB ID: 5HP3). (b) The structure of the mutant enzyme ADAR2 Q488 (PDB ID: 5ED1) also shows a hydrogen bond with N3 of the orphan cytidine.

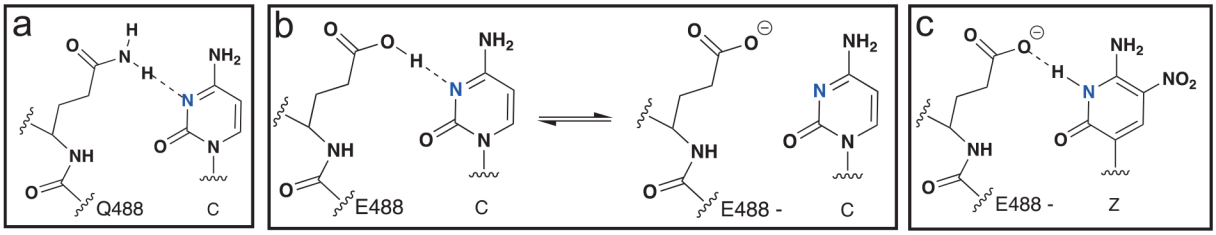

Figure 2.

(a) Protonation-independent hydrogen bond between ADAR2 Q488 and the orphan cytidine. (b) Hydrogen bond between E488 and the orphan cytidine requires protonation in order to occur. (c) Benner's base Z in the orphan position creates a protonation-independent hydrogen bond with wild-type ADAR2.

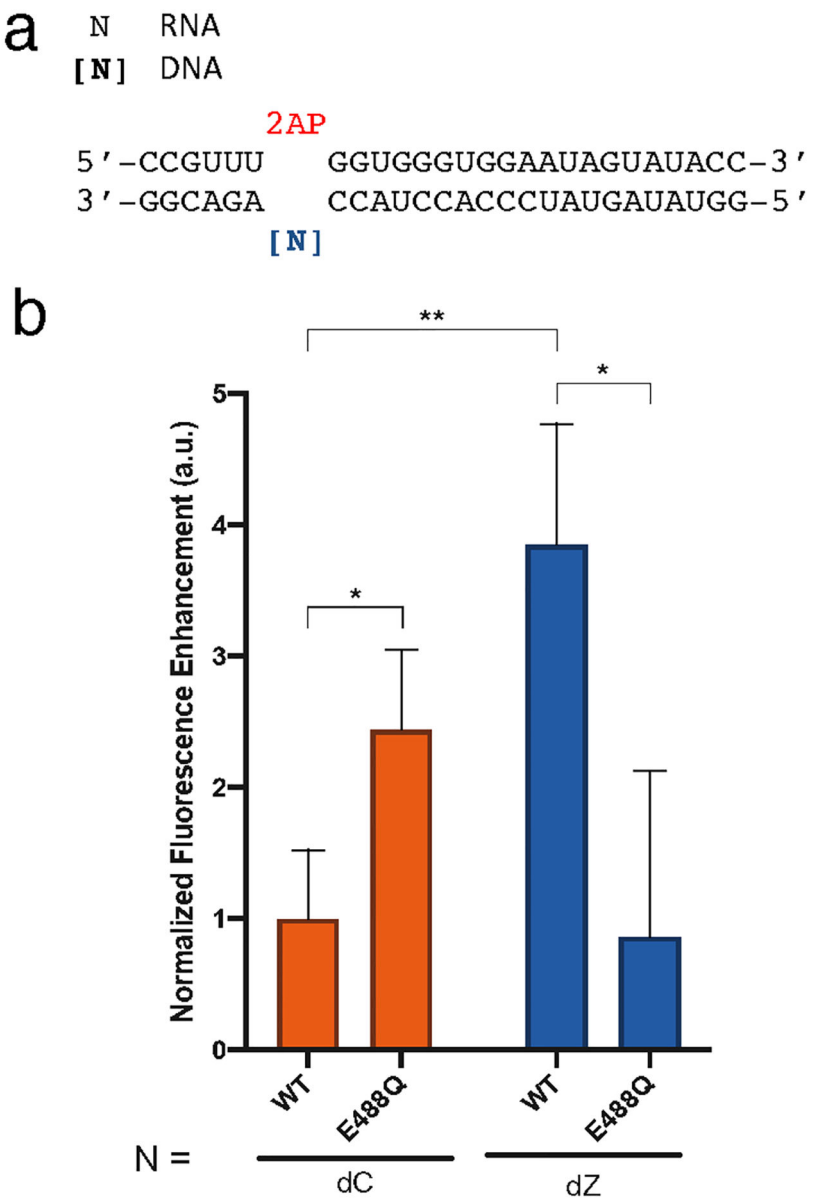

Figure 3.

(a) Substrate used in the base-flipping assay, containing 2-aminopurine (2AP) in the edited position. 2′-Deoxynucleotides are shown in brackets, and all others are ribonucleotides. The orphan base is shown as the blue N and is comprised of either 2′-deoxycytidine (dC) or 2′-deoxy Benner's base Z (dZ). (b) Plot showing normalized fluorescence enhancement for combinations of 10 μM ADAR2 wild-type or E488Q paired with 2.5 μM dsRNA containing either orphan base. Error bars represent the standard deviation of three technical replicates. Statistical significance between groups was determined using an unpaired *t* test with Welch's correction; *$p \leq 0.05$; **$p \leq 0.01$; ***$p \leq 0.001$.

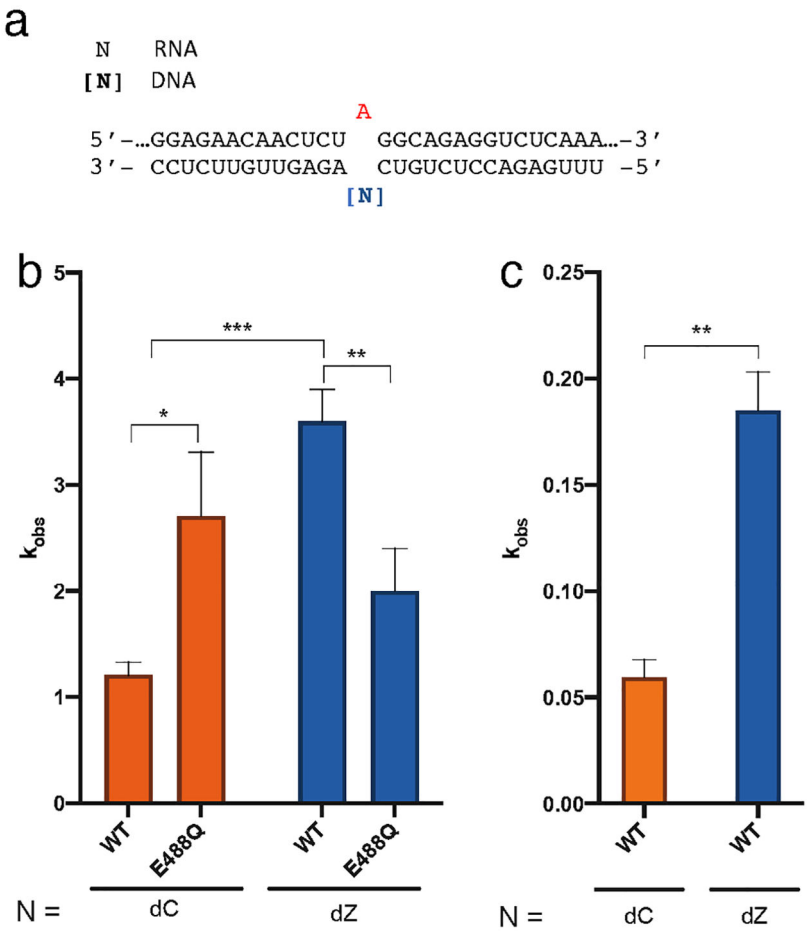

Figure 4.

(a) Partial sequence of the Idua target substrate used for in vitro deaminations, shown opposite the guide sequence. The target adenosine is shown in red, 2′-deoxynucleotides are shown in brackets, and all others are ribonucleotides. The orphan base is shown as the blue N and is either 2′-deoxycytidine (dC) or 2′-deoxy Benner's base Z (dZ). (b) Observed rate constants for the reaction of 2 nM ADAR2 wild-type (WT) or E488Q paired with 0.8 nM dsRNA substrate containing either dC or dZ in the orphan position. (c) Observed rate constants for the reaction of 50 nM ADAR1 p110 wild-type paired with 5 nM RNA substrate containing either dC or dZ in the orphan position. Error bars represent the standard deviation of three technical replicates. Statistical significance between groups was determined using an unpaired *t* test with Welch's correction; *$p \leq 0.05$; **$p \leq 0.01$.

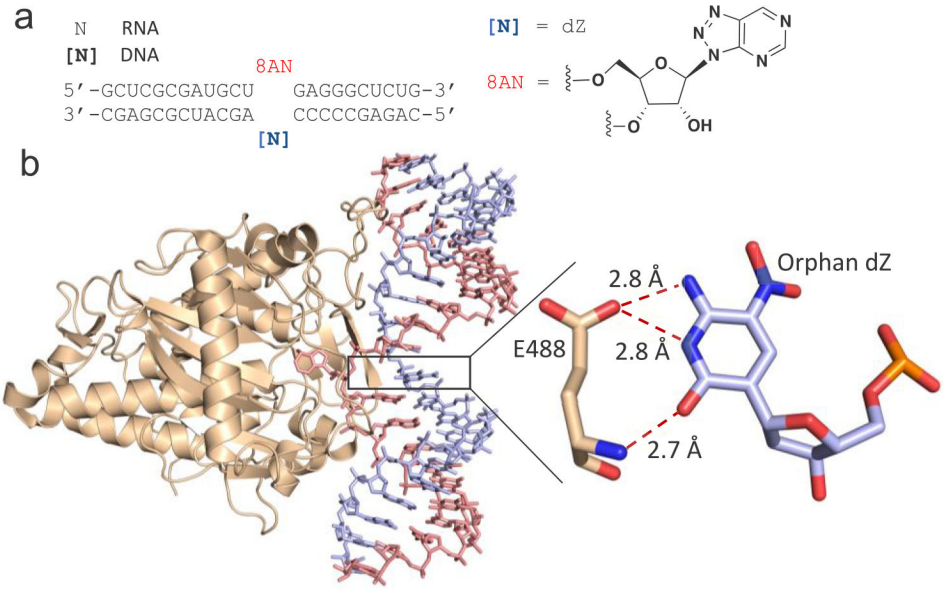

Figure 5.

(a) *GLI1* sequence duplex RNA used for crystallization. The Z base ([N]) is paired across from 8-azanebularine (8AN). (b) The crystal structure of ADAR2 deaminase domain bound to an RNA containing Benner's base dZ as the orphan base (PDB ID: 7KFN) shows enhanced hydrogen bonding contacts between the orphan base and E488.

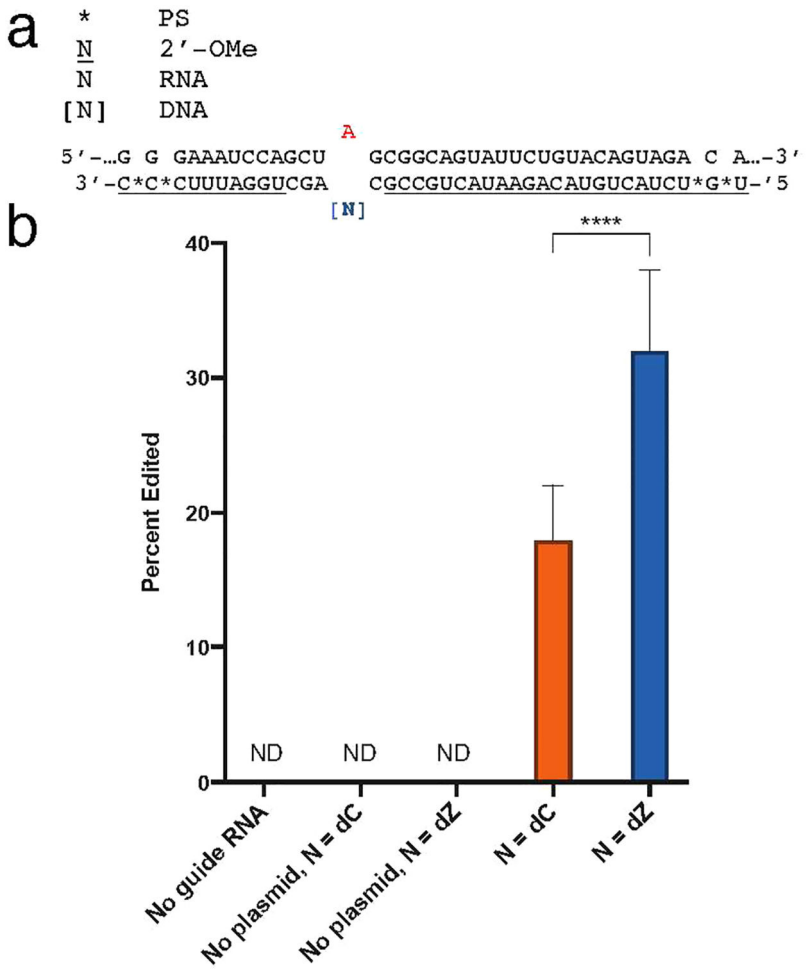

Figure 6.

(a) Partial sequence of the endogenous RAB7A transcript paired with the guide RNA. The target adenosine is shown in red. Underlining indicates 2′-*O*-methyl nucleotides, asterisks indicate phosphorothioate linkages, and nucleotides in brackets are 2′-deoxynucleotides; all others are ribonucleotides. N = cytosine or Benner's base Z. (b) Percent editing of the 3′-UTR of RAB7A with guide RNA and overexpression of ADAR2, overexpression of ADAR2 with no guide RNA, or guide RNA without ADAR2 overexpression. Percent editing values can be found in Table S5. ND indicates no detected editing. Error bars represent standard deviation ($n = 12$; 4 biological and 3 technical replicates), and statistical analysis was performed using the unpaired *t* test with Welch's correction; ****$p < 0.0001$.

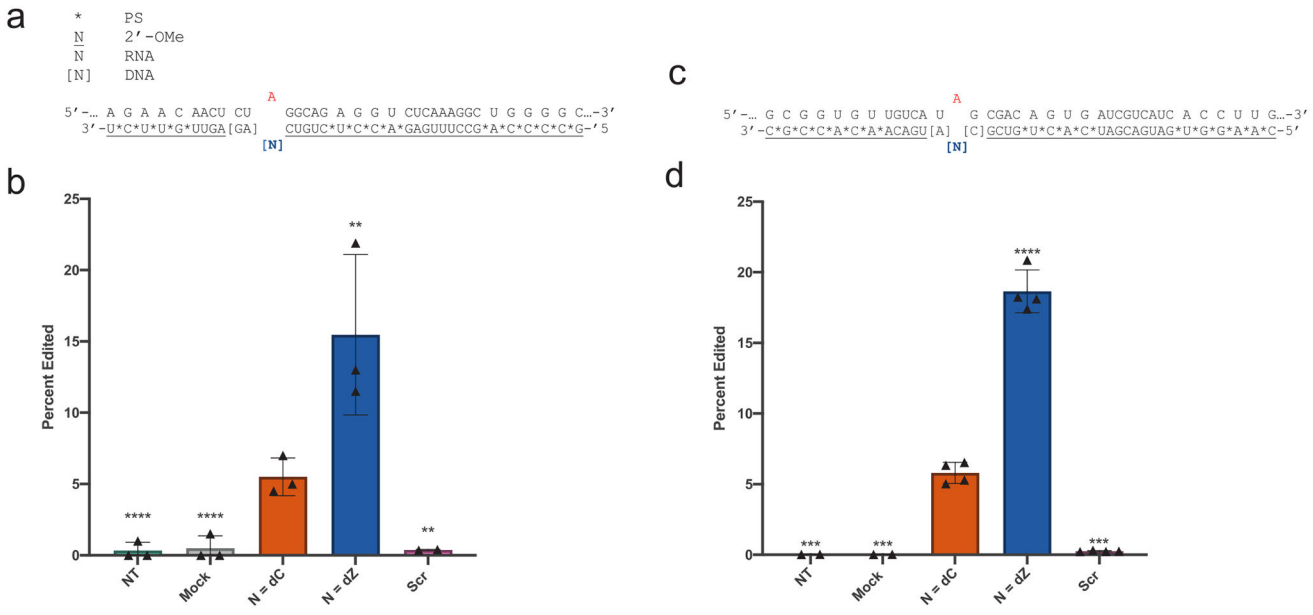

Figure 7.

(a) Partial sequence of the endogenous Idua mRNA target sequence paired with the guide oligonucleotide. The guide modifications are annotated as described in Figure 6. (b) Directed editing on the Idua RNA transcript in mouse primary liver fibroblasts. Percent editing values can be found in Table S6. NT is no transfection, and the scramble sequence (Scr) can be found in Table S7. Plotted values are the means of three biological replicates (▲) and two technical replicates ± standard deviation. The scrambled sequence (Scr) consisted of $n = 4$ measurements (2 biological and 2 technical replicates). (c) Partial sequence of the endogenous APP mRNA target sequence paired with the guide oligonucleotide. (d) Directed editing on the APP RNA transcript in ARPE-19 cells. Percent editing values can be found in Table S6. Plotted values are the means of two sets of two identical biological replicates (▲) and two technical replicates ± standard deviation. The NT and Mock conditions consisted of $n = 4$ measurements (2 biological and 2 technical replicates). Statistical significance was determined by comparing each value to the N = dC condition using the unpaired t test with Welch's correction; $n = 6$ or 8 (3 biological and 2 technical replicates; 2 sets of 2 biological and 2 technical replicates); $^{**}p \leq 0.01$; $^{***}p \leq 0.001$; $^{****}p < 0.0001$.

Table 1.

Single Turnover Rate Constants for Reaction of ADAR1/2 with Guide RNAs Containing Cytosine Analogs at the Orphan Position[a]

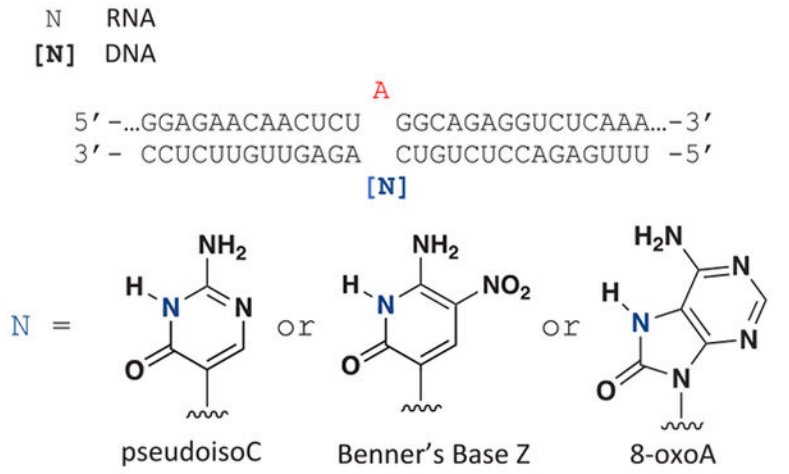

enzyme	substrate [N]	k_{obs} min^{-1}[b]	k_{rel}[c]
ADAR2	C	1.2 ± 0.1	1
	piC	1.6 ± 0.1	1.3
	Z	3.6 ± 0.3	3.0
	8-oxodA	1.4 ± 0.2	0.3
ADAR1 p110	C	0.060 ± 0.008	1
	Z	0.19 ± 0.02	3.2

[a]Reactions with ADAR2 were carried out with 0.8 nM RNA and 2 nM enzyme and for ADAR1 p110 were carried out with 5 nM RNA and 50 nM enzyme.

[b]Data were fitted to the equation $[P]t = \alpha[1 - \exp(-k_{obs} \cdot t)]$.

[c]$k_{rel} = k_{obs}$ for analog/k_{obs} for cytosine.